ISSN 1007-9327 (print)
ISSN 2219-2840 (online)

World Journal of *Gastroenterology*

World J Gastroenterol 2022 August 7; 28(29): 3753-4018

Published by Baishideng Publishing Group Inc

World Journal of Gastroenterology

Contents

Weekly Volume 28 Number 29 August 7, 2022

REVIEW

MINIREVIEWS

ORIGINAL ARTICLE

Basic Study

World Journal of Gastroenterology

Weekly Volume 28 Number 29 August 7, 2022

Contents

ABOUT COVER

Editorial Board Member of *World Journal of Gastroenterology*, Nikolaos Papadopoulos, MD, PhD, Consultant, The First Department of Internal Medicine, 417 Army Share Fund Hospital, Monis Petraki 10-12, Athens 11521, Greece. nipapmed@gmail.com

AIMS AND SCOPE

The primary aim of *World Journal of Gastroenterology* (*WJG*, *World J Gastroenterol*) is to provide scholars and readers from various fields of gastroenterology and hepatology with a platform to publish high-quality basic and clinical research articles and communicate their research findings online. *WJG* mainly publishes articles reporting research results and findings obtained in the field of gastroenterology and hepatology and covering a wide range of topics including gastroenterology, hepatology, gastrointestinal endoscopy, gastrointestinal surgery, gastrointestinal oncology, and pediatric gastroenterology.

INDEXING/ABSTRACTING

The *WJG* is now abstracted and indexed in Science Citation Index Expanded (SCIE, also known as SciSearch®), Current Contents/Clinical Medicine, Journal Citation Reports, Index Medicus, MEDLINE, PubMed, PubMed Central, Scopus, Reference Citation Analysis, China National Knowledge Infrastructure, China Science and Technology Journal Database, and Superstar Journals Database. The 2022 edition of Journal Citation Reports® cites the 2021 impact factor (IF) for *WJG* as 5.374; IF without journal self cites: 5.187; 5-year IF: 5.715; Journal Citation Indicator: 0.84; Ranking: 31 among 93 journals in gastroenterology and hepatology; and Quartile category: Q2. The *WJG*'s CiteScore for 2021 is 8.1 and Scopus CiteScore rank 2021: Gastroenterology is 18/149.

RESPONSIBLE EDITORS FOR THIS ISSUE

NAME OF JOURNAL
World Journal of Gastroenterology

ISSN
ISSN 1007-9327 (print) ISSN 2219-2840 (online)

LAUNCH DATE
October 1, 1995

FREQUENCY
Weekly

EDITORS-IN-CHIEF
Andrzej S Tarnawski

EDITORIAL BOARD MEMBERS
http://www.wjgnet.com/1007-9327/editorialboard.htm

PUBLICATION DATE
August 7, 2022

INSTRUCTIONS TO AUTHORS
https://www.wjgnet.com/bpg/gerinfo/204

GUIDELINES FOR ETHICS DOCUMENTS
https://www.wjgnet.com/bpg/GerInfo/287

GUIDELINES FOR NON-NATIVE SPEAKERS OF ENGLISH
https://www.wjgnet.com/bpg/gerinfo/240

PUBLICATION ETHICS
https://www.wjgnet.com/bpg/GerInfo/288

PUBLICATION MISCONDUCT
https://www.wjgnet.com/bpg/gerinfo/208

ARTICLE PROCESSING CHARGE
https://www.wjgnet.com/bpg/gerinfo/242

STEPS FOR SUBMITTING MANUSCRIPTS
https://www.wjgnet.com/bpg/GerInfo/239

ONLINE SUBMISSION
https://www.f6publishing.com

World Journal of Gastroenterology

Submit a Manuscript: https://www.f6publishing.com

World J Gastroenterol 2022 August 7; 28(29): 3960-3970

DOI: 10.3748/wjg.v28.i29.3960

ISSN 1007-9327 (print) ISSN 2219-2840 (online)

ORIGINAL ARTICLE

Retrospective Study

Radiomics for differentiating tumor deposits from lymph node metastasis in rectal cancer

Yong-Chang Zhang, Mou Li, Yu-Mei Jin, Jing-Xu Xu, Chen-Cui Huang, Bin Song

Specialty type: Radiology, nuclear medicine and medical imaging

Provenance and peer review: Unsolicited article; Externally peer reviewed.

Peer-review model: Single blind

Peer-review report's scientific quality classification

Grade A (Excellent): 0
Grade B (Very good): B, B
Grade C (Good): 0
Grade D (Fair): 0
Grade E (Poor): 0

P-Reviewer: Gnetti L, Italy; Hwang KH, South Korea

Received: December 29, 2021
Peer-review started: December 29, 2021
First decision: March 10, 2022
Revised: March 28, 2022
Accepted: July 6, 2022
Article in press: July 6, 2022
Published online: August 7, 2022

Yong-Chang Zhang, Department of Radiology, Chengdu Seventh People's Hospital, Chengdu 610213, Sichuan Province, China

Yong-Chang Zhang, Mou Li, Yu-Mei Jin, Bin Song, Department of Radiology, West China Hospital, Sichuan University, Chengdu 610041, Sichuan Province, China

Jing-Xu Xu, Chen-Cui Huang, Department of Research Collaboration, R&D center, Beijing Deepwise & League of PHD Technology Co., Ltd, Beijing 100080, China

Corresponding author: Bin Song, MD, PhD, Chief Doctor, Professor, Department of Radiology, West China Hospital, Sichuan University, No. 37 Guoxue Alley, Chengdu 610041, Sichuan Province, China. songlab_radiology@163.com

Abstract

BACKGROUND

Tumor deposits (TDs) are not equivalent to lymph node (LN) metastasis (LNM) but have become independent adverse prognostic factors in patients with rectal cancer (RC). Although preoperatively differentiating TDs and LNMs is helpful in designing individualized treatment strategies and achieving improved prognoses, it is a challenging task.

AIM

To establish a computed tomography (CT)-based radiomics model for preoperatively differentiating TDs from LNM in patients with RC.

METHODS

This study retrospectively enrolled 219 patients with RC [TDs^+LNM^- (n = 89); LNM^+ TDs^- (n = 115); TDs^+LNM^+ (n = 15)] from a single center between September 2016 and September 2021. Single-positive patients (*i.e.*, TDs^+LNM^- and LNM^+TDs^-) were classified into the training (n = 163) and validation (n = 41) sets. We extracted numerous features from the enhanced CT (region 1: The main tumor; region 2: The largest peritumoral nodule). After deleting redundant features, three feature selection methods and three machine learning methods were used to select the best-performing classifier as the radiomics model (Rad-score). After validating Rad-score, its performance was further evaluated in the field of diagnosing double-positive patients (*i.e.*, TDs^+LNM^+) by outlining all peritumoral nodules with diameter (short-axis) > 3 mm.

RESULTS

Rad-score 1 (radiomics signature of the main tumor) had an area under the curve (AUC) of 0.768 on the training dataset and 0.700 on the validation dataset. Rad-score 2 (radiomics signature of the largest peritumoral nodule) had a higher AUC (training set: 0.940; validation set: 0.918) than Rad-score 1. Clinical factors, including age, gender, location of RC, tumor markers, and radiological features of the largest peritumoral nodule, were excluded by logistic regression. Thus, the combined model was comprised of Rad-scores of 1 and 2. Considering that the combined model had similar AUCs with Rad-score 2 (P = 0.134 in the training set and 0.594 in the validation set), Rad-score 2 was used as the final model. For the diagnosis of double-positive patients in the mixed group [TDs^+LNM^+ (n = 15); single-positive (n = 15)], Rad-score 2 demonstrated moderate performance (sensitivity, 73.3%; specificity, 66.6%; and accuracy, 70.0%).

CONCLUSION

Radiomics analysis based on the largest peritumoral nodule can be helpful in preoperatively differentiating between TDs and LNM.

Key Words: Radiomics; Tumor deposits; Lymph node metastasis; Rectal cancer; Computed tomography; Differential diagnosis

Core Tip: In this study, a radiomics model based on the largest peritumoral nodule was developed to preoperatively differentiate tumor deposits (TDs) from lymph node (LN) metastasis in patients with rectal cancer. This model demonstrated good performance in both the training and validation cohorts. However, its performance decreased with the diagnosis of the double-positive patients. In summary, this model can be helpful for differentiating TDs from LN metastasis.

Citation: Zhang YC, Li M, Jin YM, Xu JX, Huang CC, Song B. Radiomics for differentiating tumor deposits from lymph node metastasis in rectal cancer. *World J Gastroenterol* 2022; 28(29): 3960-3970
URL: https://www.wjgnet.com/1007-9327/full/v28/i29/3960.htm
DOI: https://dx.doi.org/10.3748/wjg.v28.i29.3960

INTRODUCTION

Colorectal cancer (CRC) ranks third in terms of incidence and second in terms of mortality[1], and RC accounts for approximately 30% of CRC[2]. Tumor deposits (TDs) in RC are defined as discontinuous extramural extensions or focal aggregates of adenocarcinoma located in the perirectal region, without histological evidence of residual lymph node (LN) or vascular/neural structures[3,4]. As a factor for poor prognosis, TDs have attracted widespread attention in recent years[4,5]. A review published in 2017 confirmed that TDs were independently associated with lower overall and disease-free survival according to data available in the literature[4].

Clearly, TDs are not equivalent to LN metastasis (LNM) in terms of biology and prognosis. Among patients with LNM, the occurrence of TDs can lead to a worse prognosis[4,5], strongly indicating that their impact on prognosis is independent and additive. Therefore, TDs must be reported separately from LNM[6]. However, TDs and LNM can only be determined through pathological examinations of surgical specimens[7]. Presently, it is difficult to preoperatively differentiate TDs from LNM using computed tomography (CT).

Radiomics is a rapidly developing field of research that involves the extraction of numerous quantitative features from medical images. These features can capture characteristics of volume of interest (VOI), such as heterogeneity, and it may, alone or in combination with other data, be used to solve clinical problems[8]. Recently, some studies have reported the involvement of TDs in RC[6,9,10]. However, some previous studies did not focus on the differentiation of TDs from LNM[9,10], and Atre *et al*[6] used only texture analysis and lacked the construction and validation of a model. Therefore, we aimed to establish a CT-based radiomics model to preoperatively differentiate TDs from LNM in patients with RC.

MATERIALS AND METHODS

Patients

This retrospective study was approved by the institutional review board (No. 1159) of the authors' hospital. Given the retrospective design and use of anonymized patient data, requirements for informed consent were waived.

Patient data collected between September 2016 and September 2021 were reviewed by searching radiological and pathological databases. A total of 219 patients [single-positive, 112 male, 92 female; mean ± SD age, 60 ± 12 years (range, 32-92 years); double-positive, 6 male, 9 female; mean age, 60 ± 13 years (range, 37-83 years)] were enrolled. The inclusion criteria were as follows: Diagnosis of rectal adenocarcinoma on pathology; single positive result (*i.e.*, TDs^+ or LNM^+); and 15 randomly selected patients who were TDs^+LNM^+. The exclusion criteria were as follows: No peritumoral nodules with short-axis diameter > 3 mm on enhanced CT images (n = 22); incomplete clinical data, such as tumor markers (n = 36); patients who did not undergo surgery (n = 5); treatment before CT examination (n = 2); and poor-quality CT images (n = 4). Figure 1 shows the flow diagram of patient recruitment. Figure 2 shows the workflow of this radiomics study. Clinical characteristics, including age, gender, location of RC, tumor markers, pTN stage, extramural vascular invasion (EMVI), histological grade, and radiological features of the largest peritumoral nodule, are summarized in Table 1.

Reference standard

Pathological confirmation reports based on surgically resected specimens were obtained from the hospital's electronic medical database. From these reports, pathological information about the main tumor and peritumoral nodules (status and number of TDs and LNMs) were obtained.

Image acquisition and evaluation

Chest-abdomen-pelvis enhanced CT can detect not only the primary tumor but also suspected metastases. The main scanning parameters of CT are described in the Supplementary Table 1.

Two experiential radiologists reviewed the CT images and recorded the radiological features while blinded to clinical and pathological information. As shown in Table 1, the tumor location and radiological features of the largest peritumoral nodule, such as size, morphology, spiculation, and CT value, was confirmed by summarizing the results of these two radiologists (disagreements were resolved by consensus discussion).

Feature extraction and model-building

The reliability of the radiomics features was tested in twenty patients. The features with intra-/inter-class correlation coefficients (ICCs) > 0.75 were considered stable[11]. Thereafter, the radiologists independently segmented the main tumor and largest peritumoral nodule by manually drawing three-dimensional VOI (Figure 2). All images were resampled to pixel spacing of 1 mm in all three dimensions. Several transformation methods, such as wavelet filter and Laplace of Gaussian filter, were applied to the original images. PyRadiomics was used to extract features from the original and filtered images[12]. Figure 2 shows the types of the features. The correlation analysis was performed to remove redundant features. In detail, if the correlation coefficient between two features was > 0.4, the one with a lower coefficient was removed. Subsequently, three feature selection methods and three machine learning methods were tested to select the best performing classifier as the radiomics model (*i.e.*, Rad-score). Statistically significant factors from univariate and multivariate logistic regression analyses were used to develop the combined model.

Model evaluation

Receiver operating characteristic (ROC) curves of the models were performed to assess and compare their performance in identifying TDs^+LNM^- patients. Moreover, the performance of the models in diagnosing double-positive (*i.e.*, TDs^+LNM^+) patients were further evaluated by outlining all peritumoral nodules with short-axis diameters > 3 mm in the mixed group [TDs^+LNM^+ (n = 15); randomly selected single-positive patients from the training or validation sets (n = 15)]. If there were two different results (TD^+ or LNM^+) in all the outlined peritumoral nodules of each patient, double-positive patients were considered to be diagnosed correctly.

Statistical analysis

Statistical analyses were performed using SPSS (IBM Corporation, Armonk, NY, United States), Stata (StataCorp LP, College Station, TX, United States), and MedCalc software. In Table 1, continuous variables were analyzed using t-test or Mann-Whitney U test, and categorical variables were compared using the chi-squared test or Fisher's exact test. The areas under the curve (AUCs) of the models were compared using DeLong's test.

Table 1 Baseline and clinical characteristics of the included patients

Characteristics	TDs^+LNM^- (n = 89)	LNM^+TDs^- (n = 115)	P value	Training set (n = 163)	Validation set (n = 41)	P value
Age (mean ± SD, yr)	59 ± 12	61 ± 12	0.268	60 ± 12	60 ± 11	0.965
Gender (man/woman)	49/40	63/52	0.969	94/69	18/23	0.113
Location (middle-low/high)	65/24	74/41	0.187	107/56	32/9	0.128
Neoadjuvant therapy (+/-)	34/55	43/72	0.906	62/101	15/26	0.864
CEA (+/-) (positive ≥ 5 ng/mL)	42/47	43/72	0.159	75/88	10/31	0.012
CA19-9 (+/-) (positive ≥ 30 U/mL)	23/66	18/97	0.072	34/129	7/34	0.589
CA125 (+/-) (positive ≥ 24 U/mL)	13/76	14/101	0.611	21/142	6/35	0.767
pT stage (T1/T2/T3/T4)	0/9/70/10	4/12/93/6	0.063	4/17/127/15	0/4/36/1	0.894
pN stage (1a/1b/1c/2a/2b)	0/0/89/0/0	52/39/0/15/9	< 0.001	37/33/71/13/9	15/6/18/2/0	0.115
Histologic EMVI (+/-)	33/56	16/99	< 0.001	41/122	8/33	0.450
Histologic grade (G1/G2/G3)	1/63/25	0/76/39	0.299	0/113/50	1/26/14	0.901
Peritumoral nodule						
Shape (irregular/regular)	12/77	2/113	0.003	11/152	3/38	0.898
Spiculation (+/-)	7/82	2/113	0.077	7/156	2/39	0.871
Size (mm^2) (median)	72.7	41.2	< 0.001	54	43	0.886
CT value (HU)	61 ± 22	65 ± 23	0.258	64 ± 23	63 ± 23	0.858
Rad-score 1 (median)	0.71	0.39	< 0.001	0.44	0.71	0.002
Rad-score 2 (median)	0.89	0.13	< 0.001	0.39	0.62	0.561

Rad-score 1: Rad-score of the main tumor; Rad-score 2: Rad-score of the largest peritumoral nodule; CT: Computed tomography; TDs: Tumor deposits; LNM: Lymph node metastasis; CEA: Carcinoembryonic antigen; CA19-9: Carbohydrate antigen 19-9; CA125: Carbohydrate antigen 125; pT stage: Pathological T stage; pN stage: Pathological N stage; EMVI: Extramural vascular invasion.

RESULTS

Patient characteristics

A total of 219 patients with RC [TDs^+LNM^- (n = 89); LNM^+TDs^- (n = 115); TDs^+LNM^+ (n = 15)] were enrolled in this study. Clinical factors, including pathological N stage, pathological EMVI, and the size and shape of the largest peritumoral nodule, were found significantly different between the TDs^+LNM^- group and LNM^+TDs^- group. No statistical differences were found in age, gender, location of RC, tumor markers, pathological T stage, histological grade, and other features of the peritumoral nodule (spiculation and CT values) between the TDs^+LNM^- group and LNM^+TDs^- group. The patients were classified into a training set (n = 163) and a validation set (n = 41). Except for carcinoembryonic antigen (P = 0.012), no significant differences were found in the other clinical factors between the training and validation sets (Table 1).

Feature selection and model building

After evaluating the reliability, a large number of radiomics features remained (n = 1490 extracted from the tumor and 1252 from the largest peritumoral nodule), with ICCs of > 0.75. After excluding redundant radiomics features, we selected features using the L1-based method and established Rad-score using a logistic regression analysis. Features included in Rad-score are reported in the Supplementary Tables 2 and 3. Rad-score of the main tumor (Rad-score 1) and that of the largest peritumoral nodule (Rad-score 2) were independent risk factors for differentiating TDs from LNM [odds ratio (OR) = 3.267 and 14.396, respectively]. Regarding clinical factors, although the size and shape of the largest peritumoral nodule had significant difference between the TDs^+ group and LNM^+ group, they were all deleted in the logistic regression (P = 0.314 and 0.948, respectively; Table 2). Furthermore, a combined model integrating Rad-scores of 1 and 2 was established using the logistic regression.

Table 2 Univariate and multivariate logistic regression analysis

Variables	Univariate		Multivariate	
	OR	*P* value	OR	*P* value
Age	0.995	0.693	-	-
Gender	0.820	0.534	-	-
Location	0.819	0.282	-	-
CEA	1.546	0.171	-	-
CA19-9	1.613	0.217	-	-
CA125	1.503	0.384	-	-
Peritumoral nodule				
Shape	14.918	0.011	0.915	0.948
Spiculated (+/-)	8.400	0.051	-	-
Size (mm^2)	1.009	0.001	0.999	0.314
CT value (HU)	0.994	0.364	-	-
Rad-score 1	2.946	< 0.001	3.267	< 0.001
Rad-score 2	11.979	< 0.001	14.396	< 0.001

Rad-score 1: Rad-score of the main tumor; Rad-score 2: Rad-score of the largest peritumoral nodule; CEA: Carcinoembryonic antigen; CA19-9: Carbohydrate antigen 19-9; CA125: Carbohydrate antigen 125; CT: Computed tomography; OR: Odds ratio.

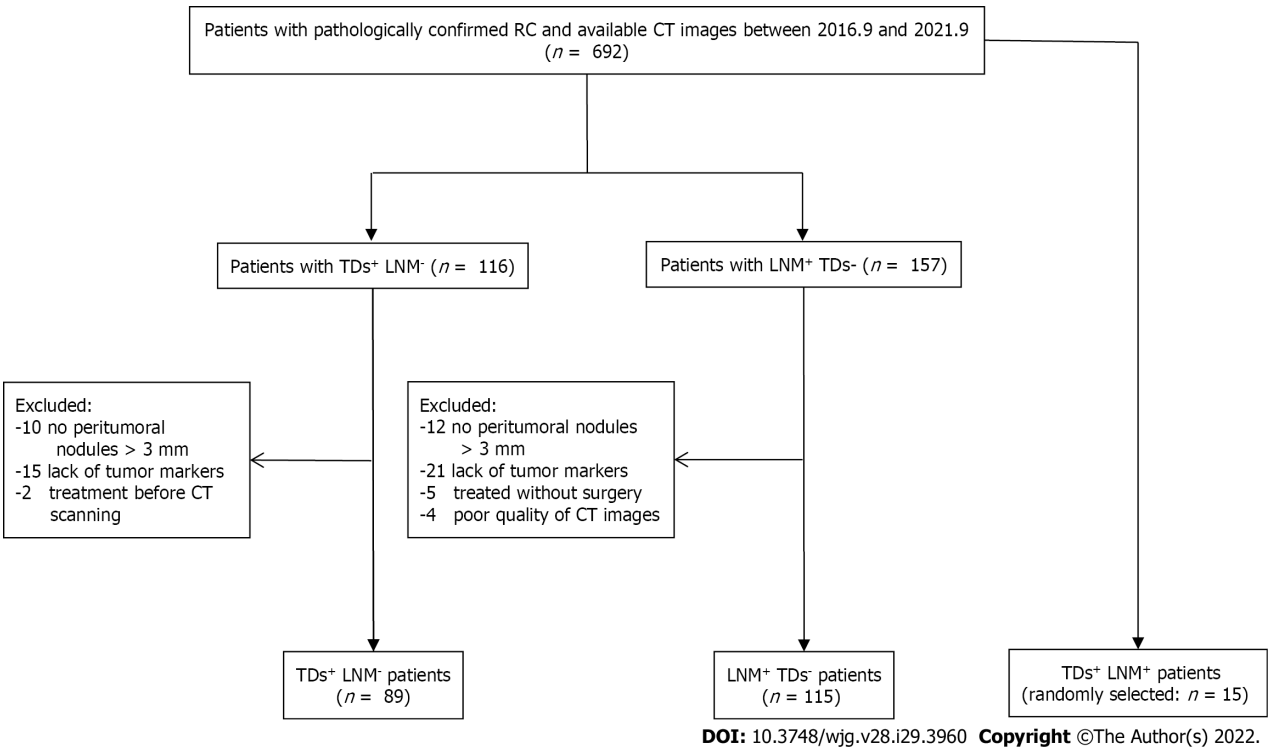

Figure 1 Flowchart of patients' recruitment pathway. RC: Rectal cancer; CT: Computed tomography; TDs: Tumor deposits; LNM: Lymph node metastasis.

Model evaluation

For classification results, the AUC for Rad-score 1 was 0.768 [95% confidence interval (CI): 0.695-0.830] in the training set and 0.700 (95%CI: 0.537-0.833) in the validation set. Rad-score 2 achieved improved performance, with an AUC of 0.940 (95%CI: 0.892-0.971) in the training set and 0.918 (95%CI: 0.789-0.981) in the validation set. The combined model (Rad-scores 1 + 2) had similar AUCs to Rad-score 2 in both the training and validation sets, as shown in Table 3 and Figure 3A and B. Thus, Rad-score 2 (Rad-

Table 3 Comparisons of the models in the training, validation, and mixed groups

	Training set				Validation set				Mixed group		
	AUC	SEN	SPE	*P* value	AUC	SEN	SPE	*P* value	SEN	SPE	Accuracy
Rad-score 1	0.768 (95%CI: 0.695-0.830)	66.2%	70.7%	< 0.001	0.700 (95%CI: 0.537-0.833)	77.8%	47.8%	0.032	-	-	-
Combined model	0.955 (95%CI: 0.910-0.981)	83.1%	88.0%	0.134	0.930 (95%CI: 0.805-0.986)	94.4%	82.6%	0.594	66.6%	73.3%	70.0%
Rad-score 2	0.940 (95%CI: 0.892-0.971)	83.1%	84.8%		0.918 (95%CI: 0.789-0.981)	83.3%	82.6%		73.3%	66.6%	70.0%

The mixed group consisted of 15 double-positive (TDs^+LNM^+) and 15 single-positive (11 TDs^+LNM^- and 4 LNM^+TDs^-) patients. *P* value: compared with Rad-score 2 by DeLong's test. Rad-score 1: Rad-score of the main tumor; Rad-score 2: Rad-score of the largest peritumoral nodule; TDs: Tumor deposits; LNM: Lymph node metastasis; AUC: Area under the curve; SEN: Sensitivity; SPE: Specificity.

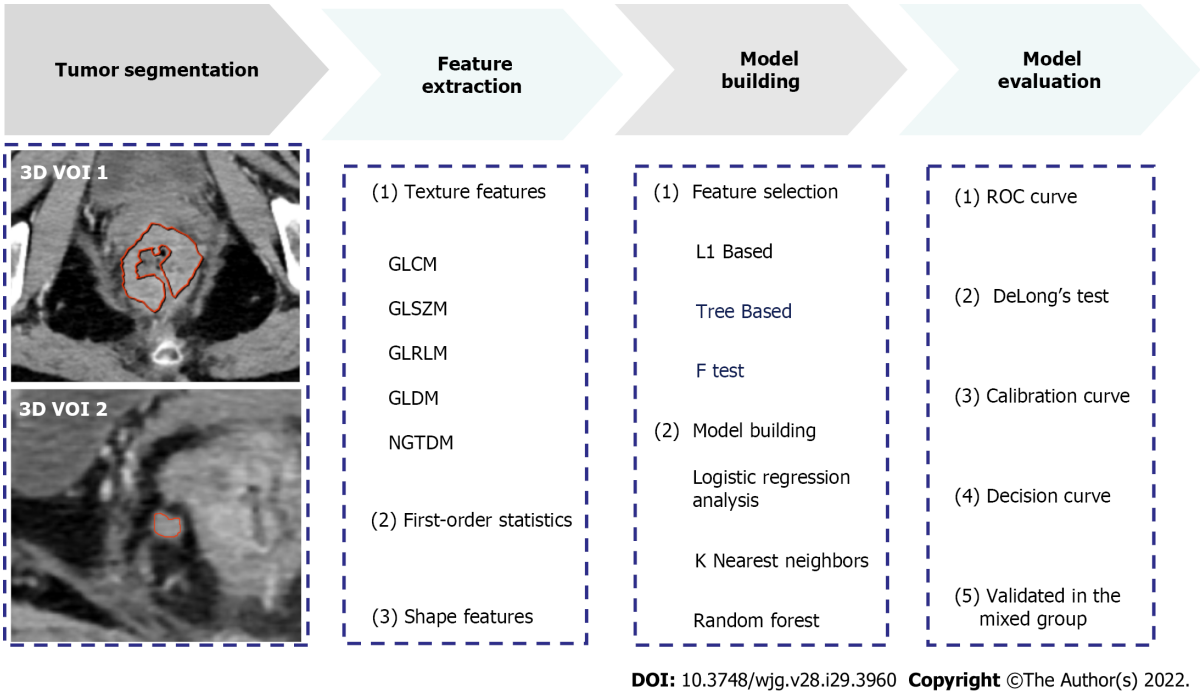

DOI: 10.3748/wjg.v28.i29.3960

Figure 2 Radiomics workflow. 3D VOI: Three-dimensional volume of interest; GLCM: Gray level co-occurrence matrix; GLSZM: Gray level size zone matrix; GLRLM: Gray level run length matrix; GLDM: Gray level dependence matrix; NGTDM: Neighbouring gray tone difference matrix; ROC: Receiver operating characteristic curve.

score of the largest peritumoral nodule) was used as the final model owing to its simplicity.

In the calibration curve for Rad-score 2, the solid line was close to the reference line (dotted line), indicating that Rad-score 2 demonstrated good agreement between the prediction (x-axis) and observation (y-axis) (Figure 3C). However, Rad-score 2 still overestimated the actual risk for TDs^+ (approximately 10%, at most). A decision curve was constructed to evaluate the clinical utility of Rad-score 2 in differentiating TDs from LNM. The net benefit can be measured along the y-axis. Figure 3D shows that Rad-score 2 yielded more benefit than "treat all", "treat none", and Rad-score 1. A case example is shown in Figure 4.

Moreover, all peritumoral nodules with short-axis diameter > 3 mm were delineated in each patient in the mixed group [TDs^+LNM^+ (n = 15); single-positive (n = 15)] to evaluate the performance of the models in predicting double-positive (*i.e.*, TDs^+LNM^+) patients. Of the 30 patients, 134 peritumoral nodules were delineated. Rad-score 2 had a moderate accuracy of 70% (sensitivity, 73.3%; specificity, 66.6%). Because the combined model had the same accuracy of 70% as Rad-score 2, it confirmed the use of Rad-score 2 as the final model.

Subgroup analysis

In view of the prognostic difference between the upper and middle-lower RC[13], we performed a subgroup analysis indicating that Rad-score 2 had high AUCs in both the upper [0.941 (95%CI: 0.853-

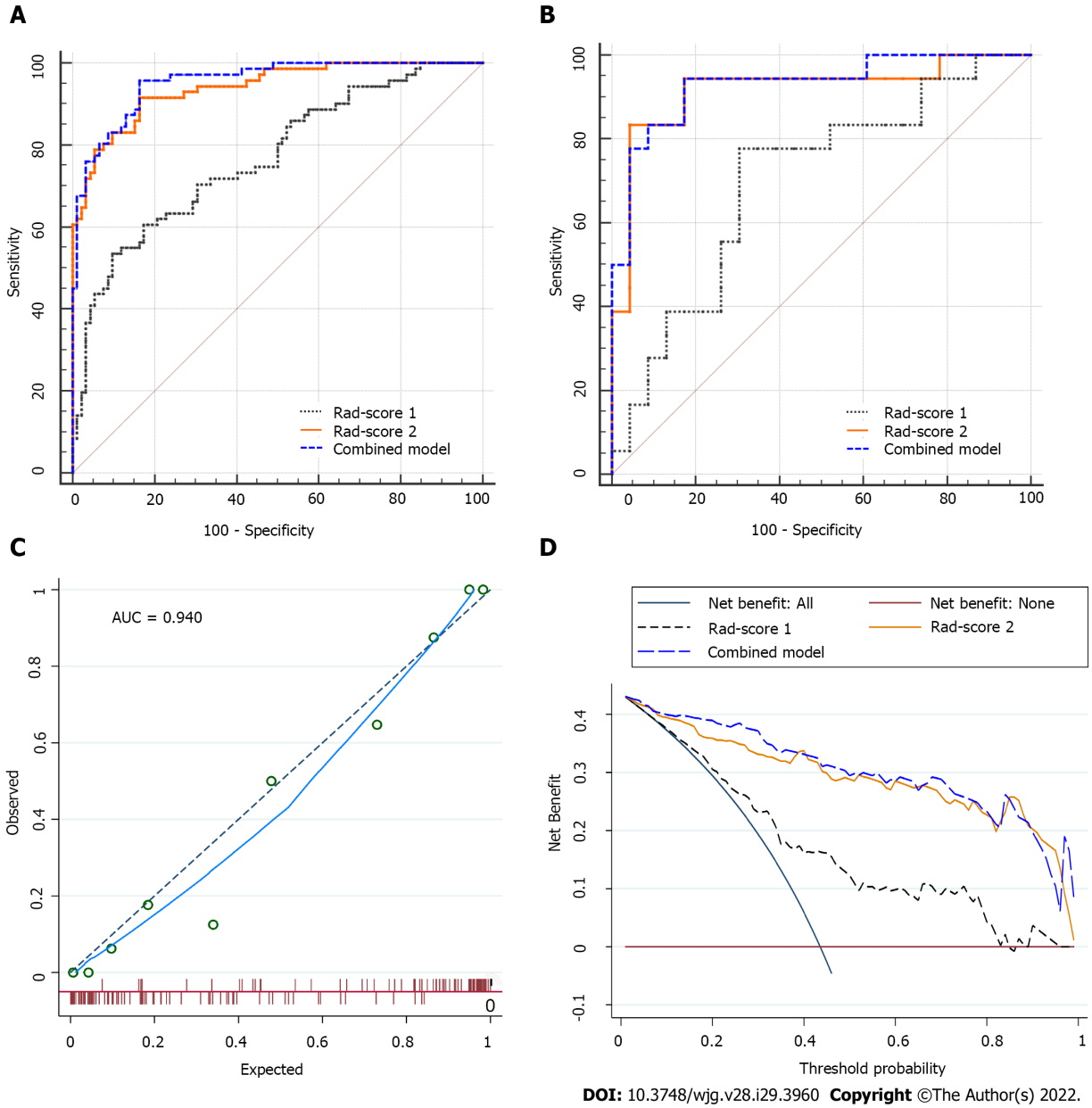

DOI: 10.3748/wjg.v28.i29.3960

Figure 3 Comparisons of the receiver operating characteristic curves, and fit and usefulness evaluation of Rad-score 2. A: In the training set: Area under the curve (AUC) = 0.768 for Rad-score 1, 0.955 for the combined model, and 0.940 for Rad-score 2; B: In the validation set: AUC = 0.700 for Rad-score 1, 0.930 for the combined model, and 0.918 for Rad-score 2; C: The calibration curve of Rad-score 2 shows good agreement between the predicted and observed risks in the training cohort; D: The decision curve demonstrates that Rad-score 2 obtains more benefit than "treat all", "treat none", and Rad-score 1. Rad-score 1: Rad-score of the main tumor; Rad-score 2: Rad-score of the largest peritumoral nodule; AUC: Area under the curve.

0.984)] and middle-lower [0.931 (95%CI: 0.875-0.967)] RC groups. For patients receiving neoadjuvant chemoradiotherapy (nCRT), Rad-score 2 also had high AUCs, as shown in Table 4. In these subgroup analyses, Rad-score 2 outperformed Rad-score 1.

The American Joint Committee on Cancer (AJCC) tumor-node-metastasis (TNM) staging system has not correlated a higher number of TDs with staging, unlike LNs (*e.g.*, N1, 1-3 and N2, ≥ 4 regional LNs) [14]. Several authors have found that patients with ≥ 3 TDs have a significantly worse prognosis than those with 1-2 TDs[15]. However, in this study, the values of Rad-scores 1 and 2 were not significantly different between the ≥ 3 TDs group and the 1-2 TDs group (P = 0.838 for Rad-score 1, and P = 0.309 for Rad-score 2) (Table 4).

DISCUSSION

Our study established a new radiomics signature (Rad-score 2) based on 11 features extracted from the largest peritumoral nodule, demonstrating the potential for preoperatively differentiating TDs from

Table 4 Subgroup analyses of the models in single-positive patients

	Rad-score 1			Rad-score 2			*P* value
Subgroups	**AUC**	**SEN (%)**	**SPE (%)**	**AUC**	**SEN (%)**	**SPE (%)**	
nCRT							
With (n = 77)	0.740 (95%CI: 0.628-0.833)	73.5%	74.4%	0.897 (95%CI: 0.806-0.954)	73.5%	90.7%	0.014
Without (n = 127)	0.753 (95%CI: 0.668-0.825)	60%	86.1%	0.957 (95%CI: 0.905-0.985)	89.1%	93.1%	< 0.001
Location							
Mid-low (n = 139)	0.782 (95%CI: 0.704-0.848)	75.4%	62.2%	0.931 (95%CI: 0.875-0.967)	86.2%	82.4%	< 0.001
High (n = 65)	0.643 (95%CI: 0.515-0.758)	54.2%	73.2%	0.941 (95%CI: 0.853-0.984)	83.3%	85.4%	< 0.001
Number of TDs	1-2 (n = 50)	≥ 3 (n = 39)	P = 0.838	1-2 (n = 50)	≥ 3 (n = 39)	P = 0.309	
Value	0.64 ± 0.24	0.65 ± 0.22		0.83 ± 0.22	0.77 ± 0.26		

Rad-score 1: Rad-score of the main tumor; Rad-score 2: Rad-score of the largest peritumoral nodule; TDs: Tumor deposits; AUC: Area under the curve; SEN: Sensitivity; SPE: Specificity; nCRT: Neoadjuvant chemoradiotherapy.

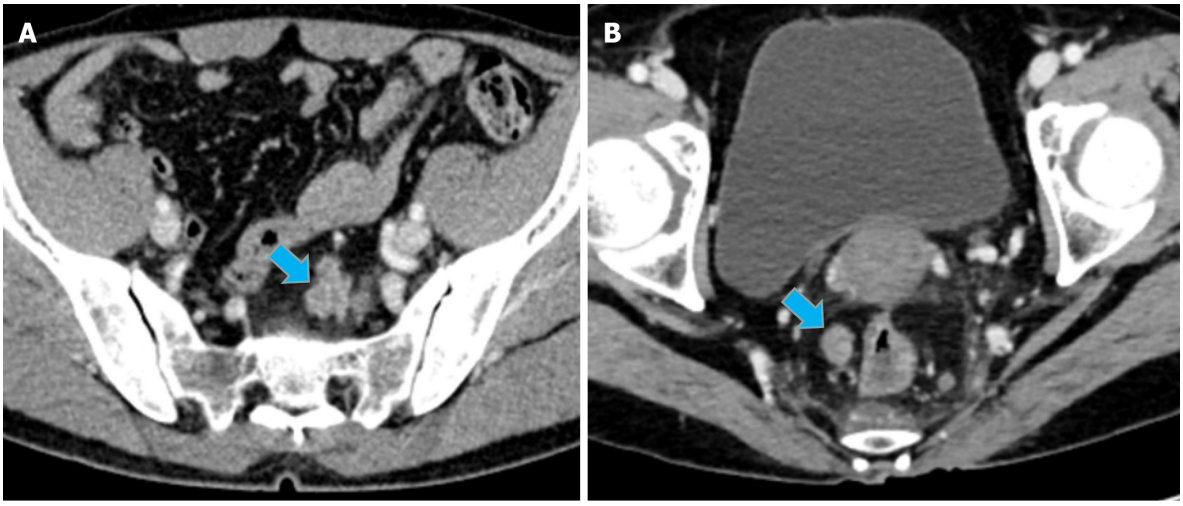

DOI: 10.3748/wjg.v28.i29.3960

Figure 4 Case presentation. A: A 56-year-old man with upper RC, the nodule of TDs (size: 24 mm × 16 mm) had an irregular shape; B: A 44-year-old man with lower RC, the nodule of TDs (size: 14 mm × 11 mm) had a regular oval shape. It is difficult to distinguish TDs and LNM from conventional imaging findings. For these two patients, Rad-score of the largest peritumoral nodule achieved correct diagnosis (values = 0.98 and 0.97, respectively). RC: Rectal cancer; TDs: Tumor deposits; LNM: Lymph node metastasis.

LNM. Moreover, Rad-score 2 outperformed Rad-score 1 (based on the main tumor) in this field [0.918 *vs* 0.700 (P = 0.032) in the validation set]. However, this model had a minor overestimation of TDs^+ probability for most of the included patients.

The 8th AJCC TNM staging system incorporates a N1c category for RC patients with TDs^+LNM^-. The N1c category represents 5% to 10% of RC with TDs (TDs^+LNM^- and TDs^+LNM^+) observed in approximately 20% of all rectal adenocarcinomas[5]. Although many authors have speculated on the origin of TDs, the phenomenon remains unclear. However, some authors have found that a significant proportion of TDs cannot be traced back to the LN[16]. Goldstein *et al*[17] reported that, after performing experiments on deeper sections, most TDs (up to 90%) exhibited signs of > 1 origin. Currently, the only method to determine the status of peritumoral nodules is the histopathologic examination of the resected specimens. The preoperative differentiation of TDs and LNM facilitates the design of individualized treatment strategies and evaluation of prognosis.

Unlike CT and magnetic resonance imaging (MRI), radiomics may solve clinical problems by extracting an enormous number of features which can quantify invisible differences in tissues for the human eye. Several radiomics studies investigating TDs[6,9,10] and LNM[18-21] have been reported in

RC. There were, however, some differences in our study. First, in contrast to most previous models (predicting single factor positive TDs[9,10] or LNM[18-21]), our model can be used to predict the status of both TDs and LNM. When a peritumoral nodule with a short-axis diameter > 3 mm was found on CT images, we could then use our model to predict the classification of this nodule (TDs^+ or LNM^+) and further identify the patient as TDs^+ only, LNM^+ only, or double positive. Second, we delineated the main tumor and the largest peritumoral nodule, while previous authors delineated the tumor and whole peritumoral fat[10] or only the main tumor[9]. Third, our study included a larger sample size of TDs^+ patients (n = 89) and had a higher AUC (0.918 in the validation set) than those reported by Chen *et al*[10] [TDs^+ (n = 40); AUC 0.795], Yang *et al*[9] [TDs^+ (n = 23); AUC 0.820], and Atre *et al*[6] [TDs^+ (n = 25); AUC 0.810]. Finally, although Atre *et al*[6] could also predict both TDs^+ and LNM^+, they only performed texture analysis, which was clearly different from the analysis in our study.

Notably, double-positive patients had a worse prognosis than those with TDs^+ or LNM^+ only. One positive LN 5-year survival rate was 62% without TDs, *vs* 44% with TDs[4]. Thus, preoperative diagnosis of double-positive patients is of great clinical significance. However, the performance of the model decreased (accuracy, 70%) when used to diagnose double-positive patients. We speculated that this may be related to the following factors. First, we established a model based on the largest peritumoral nodule. When diagnosing double-positive patients, we used all peritumoral nodules (> 3 mm). Thus, the mean size in the mixed group was smaller than that in the training set. Second, the sample size of the mixed group was small. Third, among the double-positive patients, some LNMs were incorrectly evaluated as TDs. In these lesions, the value of wavelet-HLH_firstorder_Median (a radiomics feature) decreased. In the future, we will include a larger sample to improve the applicability of the model in double-positive patients.

Nevertheless, the nature of TDs after neoadjuvant therapy remains unclear. Regarding the 77 patients who underwent nCRT in our study, the AUC for the Rad-score 2 did not decrease significantly (0.897), indicating that the model was stable. Regarding the tumor location, the AUCs of the model were also similar between the upper and middle-lower RC. Our model failed to differentiate between groups with ≥ 3 TDs and 1-2 TDs (P = 0.309).

Our study had several limitations. Firstly, because this was a retrospective study, selection bias may have been introduced. Secondly, to directly compare peritumoral nodules, we especially selected a sample comprising TDs^+LNM^- and LNM^+TDs^- and outlined the largest peritumoral nodule. However, it was still possible to identify benign peritumoral nodules. Thirdly, this was a single-center analysis. In the future, it will be necessary to conduct an external validation to confirm the versatility of the model.

CONCLUSION

A radiomics signature based on the largest peritumoral nodule is established in this article. This signature can facilitate the preoperative differentiation of TDs from LNM.

ARTICLE HIGHLIGHTS

Research background

Tumor deposits (TDs) are not equivalent to lymph node (LN) metastasis (LNM) but have become independent adverse prognostic factors in patients with rectal cancer (RC). If TDs can be differentiated from LNM before therapy, individualized treatment and patient prognosis may greatly improve.

Research motivation

Currently, preoperative differentiation of TDs and LNM can be challenging.

Research objectives

To establish a radiomics model for preoperatively differentiating between TDs and LNM in patients with RC.

Research methods

The present study retrospectively enrolled 219 patients with RC [TDs^+LNM^- (n = 89); LNM^+TDs^- (n = 115); TDs^+LNM^+ (n = 15)] from a single center between September 2016 and September 2021. Single-positive patients (TDs^+LNM^- and LNM^+TDs^-) were classified into training (n = 163) and validation (n = 41) sets. Rad-scores were established based on the main tumor and largest peritumoral nodule. After validating Rad-score, we further evaluated its performance for diagnosing double-positive patients (*i.e.*, TDs^+LNM^+) by outlining all peritumoral nodules with diameters > 3 mm (short axis).

Research results

Rad-score 1 (radiomics signature of the main tumor) had an area under the curve (AUC) of 0.768 on the training dataset and 0.700 on the validation dataset. Rad-score 2 (radiomics signature of the largest peritumoral nodule) had a higher AUC (training set: 0.940; validation set: 0.918) than Rad-score 1. For the diagnosis of double-positive patients in the mixed group [TDs^+LNM^+ (n = 15); single-positive (n = 15)], Rad-score 2 demonstrated moderate performance (sensitivity, 73.3%; specificity, 66.6%; and accuracy, 70%).

Research conclusions

The radiomics signature of the largest peritumoral nodule could provide individualized preoperative differentiation of TDs and LNM. Moreover, it was helpful in diagnosing patients who were TDs^+LNM^+.

Research perspectives

To improve the model, surgeons, radiologists, and pathologists should collaborate through prospective research to achieve node-to-node correspondence between CT images and pathological examinations in the future.

FOOTNOTES

Author contributions: Song B designed the research; Zhang YC and Jin YM collected the data; Li M, Xu JX, and Huang CC analyzed the data; Zhang YC and Li M wrote the paper; all authors have read and approved the final manuscript.

Institutional review board statement: This study was reviewed and approved by the Ethics Committee of West China Hospital of Sichuan University, No. 1159.

Informed consent statement: Patients were not required to give informed consent to the study because the analysis used anonymous clinical data that were obtained after each patient agreed to treatment by written consent.

Conflict-of-interest statement: Authors Jing-Xu Xu and Chen-Cui Huang are employed by the company Beijing Deepwise & League of PHD Technology Co., Ltd; the remaining authors declare no conflicts-of-interest related to this article.

Data sharing statement: No additional data are available.

Country/Territory of origin: China

ORCID number: Yong-Chang Zhang 0000-0003-0402-2525; Mou Li 0000-0002-7101-5942; Yu-Mei Jin 0000-0001-6606-8049; Jing-Xu Xu 0000-0003-1079-7378; Chen-Cui Huang 0000-0003-3307-6872; Bin Song 0000-0002-7269-2101.

S-Editor: Chen YL
L-Editor: A
P-Editor: Chen YL

REFERENCES

1 **Sung H**, Ferlay J, Siegel RL, Laversanne M, Soerjomataram I, Jemal A, Bray F. Global Cancer Statistics 2020: GLOBOCAN Estimates of Incidence and Mortality Worldwide for 36 Cancers in 185 Countries. *CA Cancer J Clin* 2021; **71**: 209-249 [PMID: 33538338 DOI: 10.3322/caac.21660]
2 **Bailey CE**, Hu CY, You YN, Bednarski BK, Rodriguez-Bigas MA, Skibber JM, Cantor SB, Chang GJ. Increasing disparities in the age-related incidences of colon and rectal cancers in the United States, 1975-2010. *JAMA Surg* 2015; **150**: 17-22 [PMID: 25372703 DOI: 10.1001/jamasurg.2014.1756]
3 **Maguire A**, Sheahan K. Controversies in the pathological assessment of colorectal cancer. *World J Gastroenterol* 2014; **20**: 9850-9861 [PMID: 25110416 DOI: 10.3748/wjg.v20.i29.9850]
4 **Lord AC**, D'Souza N, Pucher PH, Moran BJ, Abulafi AM, Wotherspoon A, Rasheed S, Brown G. Significance of extranodal tumour deposits in colorectal cancer: A systematic review and meta-analysis. *Eur J Cancer* 2017; **82**: 92-102 [PMID: 28651160 DOI: 10.1016/j.ejca.2017.05.027]

5 **Benoit O**, Svrcek M, Creavin B, Bouquot M, Challine A, Chafai N, Debove C, Voron T, Parc Y, Lefevre JH. Prognostic value of tumor deposits in rectal cancer: A monocentric series of 505 patients. *J Surg Oncol* 2020; **122**: 1481-1489 [PMID: 32789859 DOI: 10.1002/jso.26165]

6 **Atre ID**, Eurboonyanun K, Noda Y, Parakh A, O'Shea A, Lahoud RM, Sell NM, Kunitake H, Harisinghani MG. Utility of texture analysis on T2-weighted MR for differentiating tumor deposits from mesorectal nodes in rectal cancer patients, in a retrospective cohort. *Abdom Radiol (NY)* 2021; **46**: 459-468 [PMID: 32700214 DOI: 10.1007/s00261-020-02653-w]

7 **Jin M**, Frankel WL. Lymph Node Metastasis in Colorectal Cancer. *Surg Oncol Clin N Am* 2018; **27**: 401-412 [PMID: 29496097 DOI: 10.1016/j.soc.2017.11.011]

8 **Mayerhoefer ME**, Materka A, Langs G, Häggström I, Szczypiński P, Gibbs P, Cook G. Introduction to Radiomics. *J Nucl Med* 2020; **61**: 488-495 [PMID: 32060219 DOI: 10.2967/jnumed.118.222893]

9 **Yang YS**, Feng F, Qiu YJ, Zheng GH, Ge YQ, Wang YT. High-resolution MRI-based radiomics analysis to predict lymph node metastasis and tumor deposits respectively in rectal cancer. *Abdom Radiol (NY)* 2021; **46**: 873-884 [PMID: 32940755 DOI: 10.1007/s00261-020-02733-x]

10 **Chen LD**, Li W, Xian MF, Zheng X, Lin Y, Liu BX, Lin MX, Li X, Zheng YL, Xie XY, Lu MD, Kuang M, Xu JB, Wang W. Preoperative prediction of tumour deposits in rectal cancer by an artificial neural network-based US radiomics model. *Eur Radiol* 2020; **30**: 1969-1979 [PMID: 31828415 DOI: 10.1007/s00330-019-06558-1]

11 **Benchoufi M**, Matzner-Lober E, Molinari N, Jannot AS, Soyer P. Interobserver agreement issues in radiology. *Diagn Interv Imaging* 2020; **101**: 639-641 [PMID: 32958434 DOI: 10.1016/j.diii.2020.09.001]

12 **van Griethuysen JJM**, Fedorov A, Parmar C, Hosny A, Aucoin N, Narayan V, Beets-Tan RGH, Fillion-Robin JC, Pieper S, Aerts HJWL. Computational Radiomics System to Decode the Radiographic Phenotype. *Cancer Res* 2017; **77**: e104-e107 [PMID: 29092951 DOI: 10.1158/0008-5472.CAN-17-0339]

13 **Clancy C**, Flanagan M, Marinello F, O'Neill BD, McNamara D, Burke JP. Comparative Oncologic Outcomes of Upper Third Rectal Cancers: A Meta-analysis. *Clin Colorectal Cancer* 2019; **18**: e361-e367 [PMID: 31445919 DOI: 10.1016/j.clcc.2019.07.004]

14 **Amin MB**, Greene FL, Edge SB, Compton CC, Gershenwald JE, Brookland RK, Meyer L, Gress DM, Byrd DR, Winchester DP. The Eighth Edition AJCC Cancer Staging Manual: Continuing to build a bridge from a population-based to a more "personalized" approach to cancer staging. *CA Cancer J Clin* 2017; **67**: 93-99 [PMID: 28094848 DOI: 10.3322/caac.21388]

15 **Puppa G**, Maisonneuve P, Sonzogni A, Masullo M, Capelli P, Chilosi M, Menestrina F, Viale G, Pelosi G. Pathological assessment of pericolonic tumor deposits in advanced colonic carcinoma: relevance to prognosis and tumor staging. *Mod Pathol* 2007; **20**: 843-855 [PMID: 17491597 DOI: 10.1038/modpathol.3800791]

16 **Wünsch K**, Müller J, Jähnig H, Herrmann RA, Arnholdt HM, Märkl B. Shape is not associated with the origin of pericolonic tumor deposits. *Am J Clin Pathol* 2010; **133**: 388-394 [PMID: 20154277 DOI: 10.1309/AJCPAWOLX7ADZQ2K]

17 **Goldstein NS**, Turner JR. Pericolonic tumor deposits in patients with T3N+MO colon adenocarcinomas: markers of reduced disease free survival and intra-abdominal metastases and their implications for TNM classification. *Cancer* 2000; **88**: 2228-2238 [PMID: 10820343]

18 **Chen LD**, Liang JY, Wu H, Wang Z, Li SR, Li W, Zhang XH, Chen JH, Ye JN, Li X, Xie XY, Lu MD, Kuang M, Xu JB, Wang W. Multiparametric radiomics improve prediction of lymph node metastasis of rectal cancer compared with conventional radiomics. *Life Sci* 2018; **208**: 55-63 [PMID: 29990485 DOI: 10.1016/j.lfs.2018.07.007]

19 **Zhou X**, Yi Y, Liu Z, Zhou Z, Lai B, Sun K, Li L, Huang L, Feng Y, Cao W, Tian J. Radiomics-Based Preoperative Prediction of Lymph Node Status Following Neoadjuvant Therapy in Locally Advanced Rectal Cancer. *Front Oncol* 2020; **10**: 604 [PMID: 32477930 DOI: 10.3389/fonc.2020.00604]

20 **Li J**, Zhou Y, Wang X, Zhou M, Chen X, Luan K. An MRI-based multi-objective radiomics model predicts lymph node status in patients with rectal cancer. *Abdom Radiol (NY)* 2021; **46**: 1816-1824 [PMID: 33241428 DOI: 10.1007/s00261-020-02863-2]

21 **Zhu H**, Zhang X, Li X, Shi Y, Zhu H, Sun Y. Prediction of pathological nodal stage of locally advanced rectal cancer by collective features of multiple lymph nodes in magnetic resonance images before and after neoadjuvant chemoradiotherapy. *Chin J Cancer Res* 2019; **31**: 984-992 [PMID: 31949400 DOI: 10.21147/j.issn.1000-9604.2019.06.14]

Published by **Baishideng Publishing Group Inc**
7041 Koll Center Parkway, Suite 160, Pleasanton, CA 94566, USA
Telephone: +1-925-3991568
E-mail: bpgoffice@wjgnet.com
Help Desk: https://www.f6publishing.com/helpdesk
https://www.wjgnet.com